Protocol Article

Data on the removal of fluoride from aqueous solutions using synthesized P/γ-Fe$_2$O$_3$ nanoparticles: A novel adsorbent

Shahin Ahmadi[a,*], Somayeh Rahdar[a],
Chinenye Adaobi Igwegbe[b], Abbas Rahdar[c],
Nahid Shafighi[a], Fardin Sadeghfar[c]

[a] Department of Environmental Health, Zabol University of Medical Sciences, Zabol, Iran
[b] Department of Chemical Engineering, Nnamdi Azikiwe University, Awka, Nigeria
[c] Department of Physics, University of Zabol, Zabol, P. O. Box. 35856-98613, Islamic, Iran

A B S T R A C T

High concentration of fluoride above the optimum level can lead to dental and skeletal fluorosis. The data presents a method for its removal from fluoride-containing water. P/γ-Fe$_2$O$_3$ nanoparticles was applied as an adsorbent for the removal of fluoride ions from its aqueous solution. The structural properties of the P/γ-Fe$_2$O$_3$ nanoparticles before and after fluoride adsorption using the Fourier transform infrared (FTIR) technique were presented. The effects of pH (2–11), contact time (15–120 min), initial fluoride concentration (10–50 mg/L) and P/γ-Fe$_2$O$_3$ nanoparticles dosage (0.01–0.1 g/L) on the removal of F$^-$ on P/γ-Fe$_2$O$_3$ nanoparticles were presented with their optimum conditions. Adsorption kinetics and isotherm data were provided. The models followed by the kinetic and isotherm data were also revealed in terms of their correlation coefficients (R^2).
© 2018 The Author(s). Published by Elsevier B.V. This is an open access article under the CC BY license (http://creativecommons.org/licenses/by/4.0/).

Specifications Table

• Subject area	• Environmental Engineering
• More specific subject area	• Adsorption

---

* Corresponding author.
  E-mail address: sh.ahmadi398@gmail.com (S. Ahmadi).

• Type of data	• Image, table, and figure
• How data was acquired	• All adsorption experiments were done in batch mode. After the adsorption process, the residual fluoride concentrations were estimated. The initial and residual fluoride concentrations in the solutions were analyzed using a UV–visible recording spectrophotometer (Shimadzu Model, CE-1021-UK) at 570 nm. Fourier-transform infrared spectroscopy (FT-IR) was done on a JASCO 640 plus machine (in the range of 400-4000 cm^{-1}) to determine the functional groups present in the adsorbent before and after fluoride adsorption. The pH of the solution was measured using a MIT65 pH meter.
• Data format	• Raw and analyzed
• Experimental factors	• The influence of pH, contact time, initial fluoride concentration and P/γ-Fe$_2$O$_3$ nanoparticles dosage on the adsorption process. Kinetic and isotherm parameters were also presented.
• Experimental features	• Fluoride removal from aqueous solution using P/γ-Fe$_2$O$_3$ nanoparticles. P/γ-Fe$_2$O$_3$ nanoparticle characterization data obtained from FTIR. Kinetic and isotherm modeling of the removal process.
• Trial registration	• Not applicable
• Ethics	• Not applicable

Protocol data

- The presented data established that P/γ-Fe$_2$O$_3$ nanoparticles can be applied for the removal of fluoride with great efficiency.
- Data on the isotherm, kinetics, and effect of process variables were provided, which can be further explored for the design of a treatment plant for the treatment of fluoride-containing industrial effluents where a continuous removal is needed on a large scale.
- FTIR data for P/γ-Fe$_2$O$_3$ nanoparticles were also provided.
- The dataset will also serve as a reference material to any researcher in this field.

Description of protocol

Data

High concentration of fluoride is toxic and causes digestive disorders, fluorosis, endocrine, thyroid and liver damages, and also decreases the growth hormone [1,2]. In addition, it influences the metabolism of some elements such as calcium and potassium [3]. Fluoride must be properly reduced before its discharge to the water bodies. Adsorption can be considered as an effective method for the removal of fluoride [4,5]. The applicability of P/γ-Fe$_2$O$_3$ nanoparticles for fluoride removal was reported. Fourier transform infrared (FTIR) on the P/γ-Fe$_2$O$_3$ nanoparticles is given in Fig. 1. Fig. 2 shows the schematic illustration for the synthesis of P/γ-Fe$_2$O$_3$ nanoparticles. The functional groups present in the P/γ-Fe$_2$O$_3$ nanoparticles before and after fluoride adsorption are given in Table 1. The estimated adsorption isotherm and kinetic parameters are presented in Table 2.
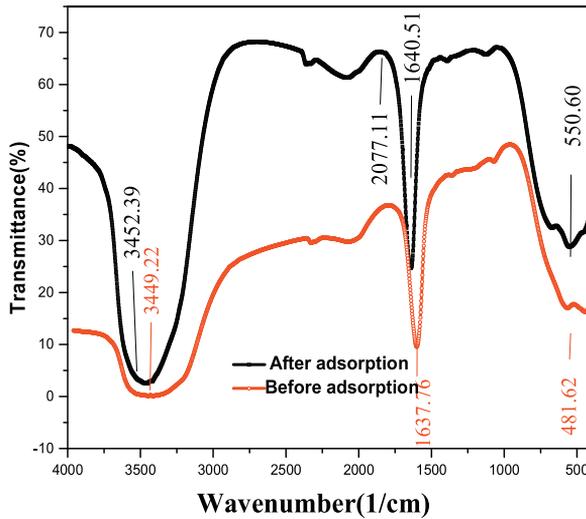
Fig. 1. FTIR spectra of the P/γ-Fe₂O₃ nanoparticles before and after fluoride adsorption.

Adsorption experiments

The adsorption experiment was conducted at batch mode using the one-factor-at-a-time (OFAT) method, that is, keeping a factor constant and varying the other factors to get the optimum condition of each variable. At first, for the purpose of this study, a stock solution of fluoride was prepared with distilled water from which other fluoride concentrations were prepared. The stock solution of fluoride (concentration of 1000 mg/L) was made by dissolving 2.21 g NaF in 1000 mL distilled water. A known mass of adsorbent (P/γ-Fe₂O₃ nanoparticles) was added to 1 L of the water samples containing different concentrations of fluoride. The pH of the water sample was adjusted by adding 0.1 N HCl or NaOH solutions. The removal efficiency was determined by varying the different adsorption process parameters such as pH (2–11), contact time (15–120 min), initial fluoride concentration (10–50 mg/L) and P/γ-Fe₂O₃ nanoparticles dosage (0.01–0.1 g/L). To create optimal conditions, the solutions were agitated using orbital shaker at a predetermined rate (150 rpm). After each experimental run, the solution was filtered and the filtrate was analyzed for the residual fluoride concentration. The initial and residual fluoride concentrations in the solutions were analyzed by a UV–vis recording spectrophotometer (Shimadzu Model: CE-1021-UK) at a wavelength of absorbance (λ_{max}): 570 nm [5].

Data analysis

The removal efficiency, R (%) and amount of fluoride adsorbed on P/γ-Fe₂O₃ nanoparticles, q_e (mg/g) of the studied parameters were estimated based on the following formulas [6–8]:

$$\%R = \frac{(C_0 - C_f)}{C_0} 100 \tag{1}$$

Where C_0 and C_f are the initial and residual fluoride concentrations (mg/g), respectively.

$$q_e = (C_0 - C_e) \times \frac{V}{M} \tag{2}$$

Where C_0 and C_e are the initial and final equilibrium liquid phase concentration of fluoride (mg/g), respectively. M is the weight of the nano adsorbent (g) and V is the volume of the solution (L).
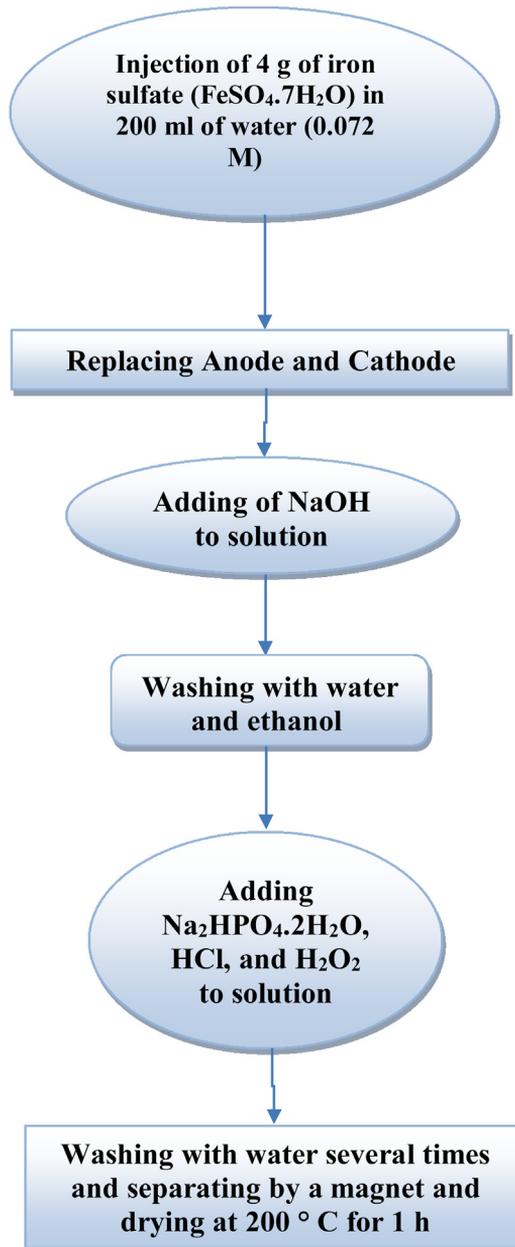
Fig. 2. The schematic illustration of the synthesis of P/γ-Fe$_2$O$_3$ nanoparticles.

Influence of process variables

In this research, the influence of pH (2 - 11), contact time (15 - 120 min), initial fluoride concentration (15 - 50 mg/L) and P/γ-Fe$_2$O$_3$ nanoparticles dosage (0.01 - 0.1 g/L) on the removal efficiency was investigated.

Table 1
Functional groups present in the P/γ-Fe$_2$O$_3$ nanoparticles before and after fluoride adsorption.

Peak (Absorbance) cm^{-1}		Type of vibration or Bond source	Functional group name	Peak intensity description
Before adsorption	After adsorption			
481.62	550.60	C—I stretch	Alkyl halides	Strong
1637.16	1640.50	N—H bend	1° amines	Medium
2025.20	2077.11	—C≡C— stretch	Alkynes	Weak
3449.22	3452.39	O—H stretch, H— bonded	Alcohols and phenols	Strong and broad

Table 2
Isotherm and kinetic data for the sorption of fluoride on P/γ-Fe$_2$O$_3$ nanoparticles.

Isotherms	Freundlich			Langmuir			Temkin		
	R^2	K_f	$1/n$	R^2	q_m	K_L	R^2	A_T	B_1
C_0(mg/L) 25	0.9	79.4	0.013	0.9999	81.3	0.012	0.995	1.19	1.088

Kinetics	Lagergren			Ho			Intraparticle diffusion		
	R^2	K_1	q_e	R^2	K_2	q_e	R^2	K_{pi}	c
C_0(mg/L) 25	0.6262	0.005	1.7	0.999	0.067	100	0.78	0.0041	97.9

Higher removal efficiency was obtained at pH of 7 (Fig. 3), an adsorbent dosage of 0.02 g/L (Fig. 4), the initial fluoride concentration of 25 mg/L (Fig. 5) and contact time of 60 min (Fig. 5). This optimum conditions of pH 7, adsorbent dosage: 0.02 g/L, contact time: 30 min and initial fluoride concentration: 25 mg/L gave an efficiency of 99% (Fig. 5).

Isotherm and kinetic modeling

An important physiochemical subject in terms of the evaluation of adsorption processes is the adsorption isotherm, which provides a relationship between the amount of fluoride adsorbed on the
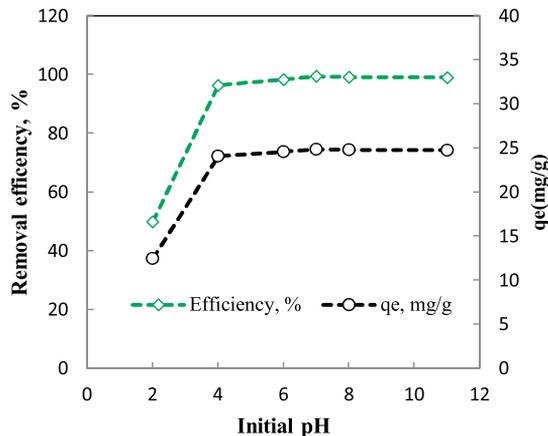

Fig. 3. Effect of pH on the removal efficiency of fluoride on P/γ-Fe$_2$O$_3$ nanoparticles.
(Contact time: 30 min, dosage: 0.09 g/L, initial fluoride concentration: 10 mg/L).
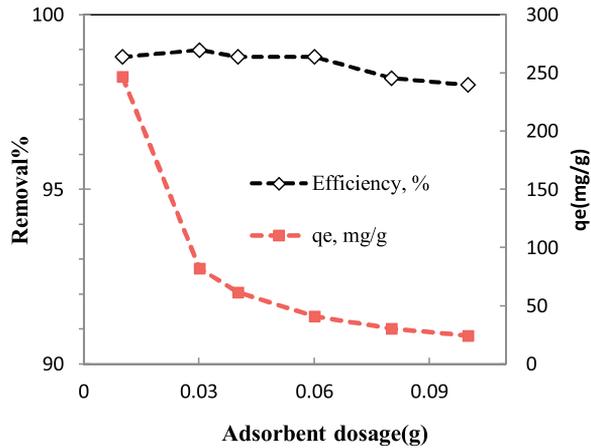
Fig. 4. Effect of adsorbent dosage on the removal efficiency of fluoride.
(Contact time: 30 min, optimum pH: 7, initial fluoride concentration: 10 mg/L).

solid phase and the concentration of fluoride in the solution when both phases are in equilibrium [9]. To analyze the experimental data and describe the equilibrium status of the adsorption between solid and liquid phases, the Langmuir, Freundlich, and Temkin isotherm models were used to fit the adsorption isotherm data.

Several kinetic models have been applied to examine the controlling mechanisms of adsorption processes such as chemical reaction, diffusion control, and mass transfer [10]. Three kinetics models, namely pseudo-first-order, pseudo-second-order, and intraparticle diffusion models were used in this study to investigate the adsorption of fluoride on P/γ-Fe_2O_3 nanoparticles.

Langmuir isotherm

For the Langmuir model, it is assumed that adsorbates attach to certain and similar sites on the adsorbent's surface and the adsorption process occurs on the monolayer surface. The Langmuir equation can be rearranged to linear form for the convenience of plotting and determining the
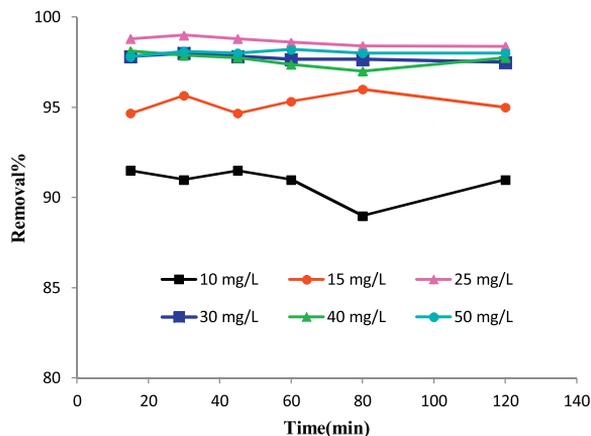

Fig. 5. Effect of initial fluoride concentration on the removal efficiency of fluoride (optimum P/γ-Fe_2O_3 nanoparticles dosage: 0.02g/L, optimum pH: 7).

isotherm constants, K_L and q_m by drawing a curve of $1/q_e$ versus $1/C_e$ [11,12]:

$$\frac{C_e}{q_e} = \frac{C_e}{q_m} + \frac{1}{q_m K_L} \tag{3}$$

Where q_e (mg/g) is the amount of fluoride adsorbed per specific amount of adsorbent, C_e is the equilibrium concentration of the fluoride solution (mg/L), K_L (L/mg) is Langmuir constant, and q_m (mg/g) is the maximum amount of fluoride required to form a monolayer.

Freundlich isotherm

The Freundlich model is an empirical relationship between the parameters, q_e, and C_e. It is obtained by assuming a heterogeneous surface with nonuniform distribution of the adsorption sites on the adsorbent surface, and can be expressed by the following equation [13,14]:

$$q_e = K_f \, C_e^{\frac{1}{n}} \tag{4}$$

Where K_f and $1/n$ are the Freundlich constants related to adsorption capacity and adsorption intensity, respectively. The Freundlich constants can be obtained by plotting a graph of Log q_e versus Log C_e based on the experimental data by applying the linear form of the Freundlich isotherm Eq. (4):

$$\log(q_e) = \log(K_f) + \frac{1}{n}\log(C_e) \tag{5}$$

Temkin isotherm

In Temkin model, the surface adsorption theory was corrected considering possible reactions between the adsorbent and adsorbate. This model can be expressed as the following equation [15]:

$$q_e = B_1 \ln(A_T) + B_1 \ln(C_e) \tag{6}$$

Where A_T and B_1 are the Temkin constants. B_1 is related to the heat of adsorption and A_T is the equilibrium binding constant.

Lagergren kinetic model

Adsorption kinetic models are used to examine the rate of adsorption process and the potential rate controlling step. The Lagergren (pseudo-first-order) rate equation is expressed as Eq. (7) [16,17]:

$$Log(q_e - q_t) = Log(q_e) - \frac{k_1}{2.303}t \tag{7}$$

Ho kinetic model

The Ho (pseudo-second-order) rate equation is given as [12,18]:

$$\frac{t}{q_t} = \frac{1}{K_2} + \frac{1}{q_e}t \tag{8}$$

Where q_e (mg g^{-1}) and q_t (mg g^{-1}) are the amounts of fluoride adsorbed at equilibrium and at time t, respectively, K_1 (min^{-1}) is the pseudo-first-order rate constant of adsorption, and K_2 (g mg^{-1} min^{-1}) is the pseudo-second-order rate constant.

Intraparticle diffusion

For the intraparticle diffusion model (Eq. (9)), c is the intercept (mg/g) and K_{pi} is the slope. If intraparticle diffusion is involved in the adsorption process, then the plot of $t_{0.5}$ versus q_t would result
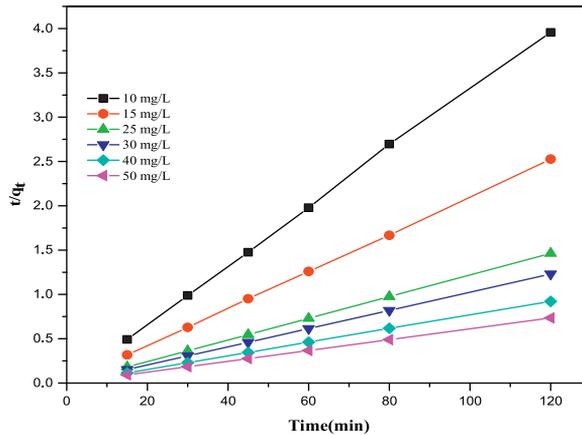
Fig. 6. Pseudo-second-order (Ho) kinetic plot for fluoride removal on P/γ-Fe$_2$O$_3$ nanoparticles.

in a linear relationship, and the intraparticle diffusion would be the controlling step if this line passed through the origin (C = 0). When the plots do not pass through the origin (C ≠ 0), this is indicative of some degree of boundary layer control and this further shows that the intraparticle diffusion is not the only rate controlling step, but also other processes may control the rate of adsorption [19,20].

$$q_t = K_{pi}t^{0.5} + c \tag{9}$$

Where q_t (mg/g) is the amount of fluoride adsorbed at time t (min) and K_{pi} (mg/g min) is the intraparticle diffusion model rate constant.

The estimated adsorption isotherm and kinetic parameter are presented in Table 2. Fig. 6 shows the adsorption kinetic (Ho) plot for fluoride removal on P/γ-Fe$_2$O$_3$ nanoparticles. The removal of fluoride on P/γ-Fe$_2$O$_3$ nanoparticles followed the Ho kinetic model with a correlation coefficient (R^2) of 0.999 at 25 mg/L, suggesting that the rate-limiting step is a chemical adsorption process [21]. The isotherm data fitted into the Freundlich, Langmuir and Temkin isotherms but fitted more to the Langmuir isotherm, which indicates a monolayer adsorption on a homogeneous surface [14].

Funding sources

Acknowledgments

References

[1] A. Rahmani, K. Rahmani, S. Dobaradaran, A.H. Mahvi, R. Mohamadjani, H. Rahmani, Child dental caries in relation to fluoride and some inorganic constituents in drinking water in Arsanjan, Iran, Fluoride 43 (2010) 179–186.

[2] S. Dobaradaran, F. Fazelinia, A.H. Mahvi, V. Hosseini, Particulate airborne fluoride from an aluminum production plant in Arak, Iran, Fluoride 42 (2009) 228–232.

[3] M.H. Dehghani, M. Faraji, A. Mohammadi, H. Kamani, Optimization of fluoride adsorption onto natural and modified pumice using response surface methodology: isotherm, kinetic and thermodynamic studies, Korean J. Chem. Eng. 34 (2017) 454–462.

[4] M. Ravanipour, R. Kafaei, M. Keshtkar, S. Tajalli, N. Mirzaei, B. Ramavandi, Fluoride ion adsorption onto palm stone: optimization through response surface methodology, isotherm, and adsorbent characteristics data, Data Brief 12 (2017) 471–479.

[5] M. Mahramanlioglu, I. Kizilcikli, I. Bicer, Adsorption of fluoride from aqueous solution by acid treated spent bleaching earth, J. Fluorine Chem. 115 (2002) 41–47.

[6] S. Ahmadi, F. Kord Mostafapour, Treatment of textile wastewater using a combined coagulation and DAF processes, Iran, 2016, Arch. Hyg. Sci. 6 (2017) 229–234.

[7] S. Ahmadi, F.K. Mostafapour, Survey of efficiency of dissolved air flotation in removal penicillin G from aqueous solutions, Br. J. Pharm. Res. 15 (2017) 1–11.

[8] S. Ahmadi, A. Banach, F.K. Mostafapour, D. Balarak, Study survey of cupric oxide nanoparticles in removal efficiency of ciprofloxacin antibiotic from aqueous solution: adsorption isotherm study, Desal. Water Treat. 89 (2017) 297–303.

[9] N. Khoshnamvand, E. Bazrafshan, B. Kamarei, Fluoride removal from aqueous solutions by NaOH-modified Eucalyptus leaves, J. Environ. Health Sustain. Dev. 3 (2018) 481–487.

[10] S. Karthikeyan, B. Sivakumar, N. Sivakumar, Film and pore diffusion modeling for adsorption of reactive red 2 from aqueous solution on to activated carbon prepared from bio-diesel industrial waste, E-J. Chem. 7 (2010) S175–S184.

[11] S. Ahmadi, C.A. Igwegbe, Adsorptive removal of phenol and aniline by modified bentonite: adsorption isotherm and kinetics study, Appl. Water Sci. 8 (2018) 170.

[12] E. Bazarafshan, S. Ahmadi, Efficiency of combined processes of coagulation and modified activated bentonite with sodium hydroxide as a biosorbent in the final treatment of leachate: kinetics and thermodynamics, J. Health Res. Commun. 3 (2017) 6-6.

[13] N. Khoshnamvand, S. Ahmadi, F.K. Mostafapour, Kinetic and isotherm studies on ciprofloxacin adsorption using magnesium oxide nanoparticles, J. App. Pharm. Sci. 7 (2017) 079–083.

[14] C.A. Igwegbe, P.C. Onyechi, O.D. Onukwuli, I.C. Nwokedi, Adsorptive treatment of textile wastewater using activated carbon produced from *Mucuna pruriens* seed shells, World J. Eng. Technol. (2016) 21–37.

[15] C.A. Igwegbe, A.M. Banach, S. Ahmadi, Adsorption of Reactive Blue 19 from aqueous environment on magnesium oxide nanoparticles: kinetic, isotherm and thermodynamic studies, Pharm. Chem. J. 5 (2018) 111–121.

[16] P. Salaryan, F. Mokari, M. Saleh Mohammadnia, M. Khalilpour, The survey of linear and non-linear methods of pseudo-second-order kinetic in adsorption of Co (II) from aqueous solutions, Int. J. Water Wastewater Treat. 1 (2013) 130–134.

[17] Sh. Ahmadi, F. Kord Mostafapour, Tea wastes as a low cost adsorbent for the removal of COD from landfill leachate: kinetic study, J. Sci. Eng. Res. 4 (2017) 103–164.

[18] L.D. Hafshejani, S. Tangsir, E. Daneshvar, M. Maljanen, A. Lähde, J. Jokiniemi, M. Naushad, A. Bhatnagar, Optimization of fluoride removal from aqueous solution by Al$_2$O$_3$ nanoparticles, J. Mol. Liq. 238 (2017) 254–262.

[19] Y. Miyah, A. Lahrichi, M. Idrissi, S. Boujraf, H. Taouda, F. Zerrouq, Assessment of adsorption kinetics for removal potential of Crystal Violet dye from aqueous solutions using Moroccan pyrophyllite, J. Assoc. Arab. Univ. Basic Appl. Sci. 23 (2017) 20–28.

[20] W.J. Weber, J.C. Morris, Kinetics of adsorption on carbon from solution, J. Sanit. Eng. Div. Am. Soc. Civil Eng. 89 (1963) 31–39.

[21] C.A. Igwegbe, O.D. Onukwuli, J.T. Nwabanne, Adsorptive removal of vat yellow 4 on activated *Mucuna pruriens* (velvet bean) seed shells carbon, Asian J. Chem. Sci. 1 (2016) 1–16.